Energy dependence of ^{24}Mg($\vec{p}$,d) cross section and analyzing-power measurements from 50 to 150 MeV

D. W. Miller, J. D. Brown,* D. L. Friesel, W. W. Jacobs, W. P. Jones, H. Nann, and P. Pichardo
Department of Physics, Indiana University, Bloomington, Indiana 47405

J. Q. Yang
Institute of Nuclear Research, Academia Sinica, Shanghai, China

P. W. F. Alons and J. J. Kraushaar
Department of Physics, University of Colorado, Boulder, Colorado 80309
(Received 12 August 1985)

Detector telescope measurements of cross sections and analyzing powers for the ^{24}Mg($\vec{p}$,d) reaction to states of ^{23}Mg up to 4.36 MeV in excitation are reported for bombarding energies of 49.2 and 150.3 MeV. Taken together with earlier spectrometer measurements at 94.8 MeV at the same laboratory, a smooth energy dependence of the results for transitions leading to $\frac{1}{2}^+$, $\frac{1}{2}^-$, $\frac{3}{2}^-$, $\frac{3}{2}^+$, $\frac{5}{2}^+$, and $\frac{7}{2}^+$ states is obtained. Exact finite-range, adiabatic, distorted-wave analyses give reasonable fits in most cases to the cross-section angular distributions using an rms radius prescription for the bound-state geometry, and the energy-dependent set of proton optical potentials employed by Hatanaka extrapolated to higher energies; however, the calculated analyzing powers often differ in magnitude and shape from experiment. With the exception of the $l_n=0$ transitions, spectroscopic factors derived from this particular comparison exhibit only a relatively small energy dependence.

I. INTRODUCTION

Experimental measurements of (p,d) reaction cross sections and analyzing powers have been extended in the past few years to medium energies using accelerators with high quality beams in this energy range. Early analyses of results obtained for $l_n=0$ transitions raised substantial questions regarding the applicability of standard DWBA methods to this reaction at or above 100 MeV.[1] The purpose of the present investigation was to study, as a function of bombarding energy, transitions involving several different neutron orbital angular momentum (l_n) and spin (j_n) transfers in order to provide a data base for detailed theoretical investigations of the energy dependence of the reaction mechanism.

The (p,d) reaction has been fairly successful as a spectroscopic tool in the energy range below 35 MeV, providing information on both the l_n and j_n of the picked-up neutron [derived from the shapes of the measured differential cross section $\sigma(\theta)$ and analyzing power $A_y(\theta)$, respectively], and on the spectroscopic factor (obtained from comparison of calculation with the magnitude of the measured cross section). Several investigations[2-5] at the Indiana University Cyclotron Facility (IUCF) have shown that the (p,d) reaction is useful for l_n and j_n determinations near 95-MeV bombarding energy as well. In particular, an empirical technique of determining shapes of $\sigma(\theta)$ and $A_y(\theta)$ for known l_n and j_n transfers and applying them as "experimental templates" to study unknown cases has been shown to be successful. The latter result is of interest because this reaction can be employed at these bombarding energies to study the nature of deep-hole states in spite of substantial negative Q values.

The original attempt by Shepard *et al.*[1] to obtain good DWBA descriptions of the results[2,3] for $l_n=0$ transfers in the ^{24}Mg($\vec{p}$,d) reaction at 94.8 MeV was not successful in spite of the inclusion of many refinements. Predictions which were in agreement with experiment could only be obtained by the artificial means of cutting off the nuclear interior, either through the use of arbitrary radial cutoffs, or by greatly increasing the absorption in the optical potentials.[1] Other approaches[6,7] also could not remove the discrepancy, although a first attempt using a Dirac formalism[8] seemed to be promising because it had the effect of suppressing contributions from the nuclear interior. Hence, in spite of subsequent analyses[9,10] showing improved fits using the adiabatic approximation,[11] there remains concern whether the nuclear interior is being treated correctly in distorted-wave calculations.

Because of the above evidence for a possible breakdown of DWBA descriptions at around 100-MeV bombarding energy, the present investigation was undertaken to obtain experimental results for one reaction over a wide energy range in the hope that future analyses might trace the onset of these difficulties. Transitions believed to be predominantly one step $l_n=0$, 1, and 2 pickup were measured, along with one transition assumed to be nondirect in character. Independently, Hatanaka *et al.*[9] undertook similar measurements at 65 and 80 MeV bombarding energy, but have reported only the results of the $l_n=2$ ground-state transition and the $l_n=0$ transitions to states at 2.36 and 4.36 MeV.

The present paper reports differential cross-section and analyzing-power results obtained at bombarding energies of 49.2 and 150.3 MeV at IUCF for the ^{24}Mg($\vec{p}$,d) reaction leading to the known low-lying $\frac{1}{2}^+$, $\frac{1}{2}^-$, $\frac{3}{2}^-$, $\frac{3}{2}^+$, $\frac{5}{2}^+$, and $\frac{7}{2}^+$ states of ^{23}Mg. A few measurements were also made at 95 MeV to provide a cross check of these detector telescope data with the earlier 95-MeV spectrometer results.[2,3] An analysis of the data for the lowest $\frac{1}{2}^+$ and $\frac{5}{2}^+$ states, incorporating results from a number of other laboratories from 27- to 185-MeV bombarding energy, has already been published.[10]

Experimental procedures used in this investigation are described in Sec. II, and the results presented in Sec. III. Section IV reviews empirical results for the j dependence of the analyzing powers for the (p,d) reaction observed from 50 to 400 MeV, and includes a qualitative explanation of the trends of these data with target mass and bombarding energy. A comparison of the results of the present experiment with adiabatic distorted-wave calculations is presented in Sec. V.

II. EXPERIMENTAL PROCEDURE

Polarized protons from an atomic-beam source located in the 800-kV electrostatic terminal at IUCF were accelerated through the injector and main cyclotrons to energies of 49.2, 94.4, and 150.3 MeV. Momentum-analyzed polarized beams of 5 to 40 nA were focused onto self-supporting rolled targets of thickness 6.51 and 10.6 mg/cm^2 enriched to 99.94% in ^{24}Mg. The reaction-product deuterons were detected in a three-element detector telescope mounted in the 1.6-m diameter scattering chamber. Since the available quadrupole-dipole-dipole-multipole (QDDM) magnetic spectrometer could be used for deuterons only up to 120 MeV, the same telescope and geometry were used for all three bombarding energies and all measurements were made in succession in order to ensure consistent results.

The three elements of the telescope were a 2-mm thick Si surface barrier detector as the first element, followed by high-purity Ge detectors[12] of thicknesses 12.0 and 13.0 mm, respectively. At 49.2 and 94.4 MeV, reaction deuterons of interest stopped in the second detector element; at 150.3 MeV they were stopped in the third. A 3.2-mm wide$\times$10.0-mm high collimator with rounded corners and a total thickness of 2.54 cm was located 56 cm from the target in front of the first detector, subtending a solid angle of 0.0942 msr. The overall (full width at half maximum) resolution of the system including target thickness, kinematic spread, and the detector and electronics was about 200 keV at 49.2 MeV and 300 keV at 150.3 MeV. Deuterons in the telescope were identified on line with software cuts utilizing the data acquisition program RAQUEL.[13]

Data were taken with the telescope described above operated in a "single-arm" mode, with the ($\vec{p}$,d) analyzing power $A_y(\theta)$ calculated from yields obtained for the two proton spin orientations normal to the reaction plane. The proton spin was reversed once a minute to reduce systematic errors associated with any slowly varying beam parameters. Beam polarization was monitored by scattering protons at 112° laboratory angle in a two-arm ^{4}He polarimeter, which was periodically inserted directly after the injector cyclotron (E_p=4.6, 8.3, and 12.1 MeV for the three bombarding energies of 49.2, 94.4, and 150.3 MeV, respectively). A very slow increase in beam polarization was noted over the six day run. Beam polarizations determined from the low-energy polarimeter during this experiment varied from about 71% to 78%. Other measurements[14] have shown that changes in polarization caused by acceleration in the main cyclotron are typically a few percent at most. This introduces errors comparable to the statistical and systematic precision obtained during the present measurements; no corrections to the data for this effect were made.

Differential cross-section and analyzing-power measurements were obtained with the 6.51-mg/cm^2 target every 2° or 3° from 7° to 40° in the laboratory system at 49.2 MeV, and with the 10.6-mg/cm^2 target from 7° to 36° at 150.3 MeV. At 94.4 MeV, measurements were made at 20°, 23°, and 26° to check against the earlier QDDM spectrometer measurements at 94.8 MeV,[2] and to compare yields from the two targets. The beam intensity on target was adjusted so as to keep the total dead time of the system to 10% or less.

Spectra were analyzed off line using the modified peak-fitting program FITIT.[15] Although some deuteron groups were not well resolved at 150 MeV, their peak locations are well known and reliable peak stripping was achieved in nearly all cases. The ratios of the yields obtained with the telescope at E_p=94.4 MeV to those obtained in the earlier 94.8-MeV spectrometer measurements[2,3] were 1.039 and 0.930, respectively, for the thinner and thicker targets used in this experiment. Therefore, to within the $\pm$15% error in the absolute cross section quoted in the earlier work, there is no evidence of particle loss in the telescope at 94.4 MeV due to outscattering or reaction processes. Since any such effects should be much less at 49.2 MeV, the present results are estimated to have an overall normalization uncertainty of $\pm$15% at 49.2 MeV. However, since no method was available for calibrating the efficiency of the telescope at 150.3 MeV, the absolute uncertainty in the results at this energy are estimated to be $\pm$30% based upon measurements with a similar telescope using recoil deuterons up to 105 MeV,[16] and upon calculated reaction probabilities in germanium up to 150 MeV.[17] Due to the tight collimation of the deuterons compared to the 2.5-cm diameter of the Ge detectors, outscattering corrections are believed to be small. The absolute cross sections obtained with the telescope at 150 MeV also fit in fairly smoothly between the earlier spectrometer results at 94.8 MeV (Ref. 2) and 185 MeV (Ref. 18).

III. EXPERIMENTAL RESULTS

A deuteron spectrum observed with the QDDM spectrometer for the ^{24}Mg(p,d)^{23}Mg reaction at 95-MeV bombarding energy has been published previously.[2] Results are only reported here for those low-lying groups which could be resolved satisfactorily in the present telescope experiment, along with the corresponding results from the

earlier 95-MeV measurements for comparison. These include groups leading to the two $\frac{1}{2}^+$ states (2.36 and 4.36 MeV), as well as to the low-lying $\frac{1}{2}^-$ (2.77 MeV), $\frac{3}{2}^-$ (3.80 MeV), $\frac{3}{2}^+$ (ground state), $\frac{5}{2}^+$ (0.45 MeV), and $\frac{7}{2}^+$ (2.05 MeV) states. Some tentative spectroscopic factor information is also reported for the $\frac{3}{2}^+$ state at 2.91 MeV which was poorly resolved.

Figures 1–4 present the cross-section and analyzing-power results for groups leading to all of the above states at 49.2-, 94.8-, and 150.3-MeV bombarding energy, plotted as a function of momentum transfer (q). Data for all but the 2.05- and 4.36-MeV states are replotted as a function of center-of-mass angle (θ) in Figs. 5–7, where comparisons with distorted-wave analyses are made. The results are displayed in these two ways to provide some qualitative indication whether diffractionlike effects appear in the observed energy dependence of the results.

A comparison of Figs. 1 and 5 for the $l_n=0$ transitions shows that the main oscillatory features of both the cross sections and the analyzing powers are reasonably stable when plotted against angle, but shift substantially when plotted against momentum transfer. It is to be noted that the distinctive positive maximum between 15° and 20° c.m. in the analyzing power rises smoothly from about 0.4

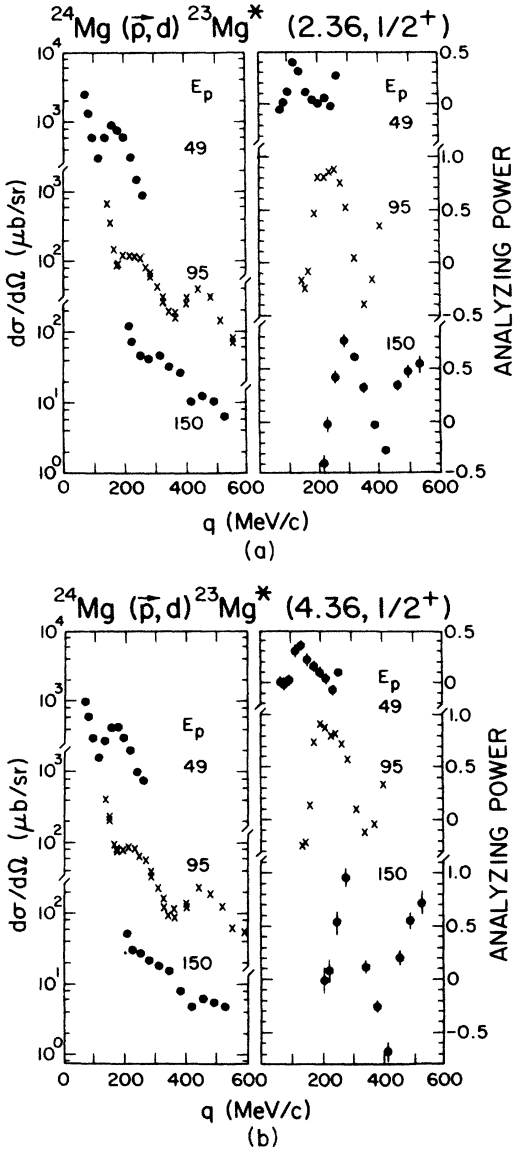

FIG. 1. Differential cross-section and analyzing-power angular distributions as a function of momentum transfer in MeV/c for the two known $l_n=0$, $j^\pi=\frac{1}{2}^+$ transitions to low-lying states in ^{23}Mg at 2.36 and 4.36 MeV, plotted at the top and bottom, respectively. The indicated error bars are purely statistical; where not shown they are smaller than the plotted points. Telescope measurements taken in this experiment at beam energies of 49.2 and 150.3 MeV are shown at the top and bottom of each figure, and the previously-published 94.8-MeV spectrometer results (Ref. 2) are displayed in the center.

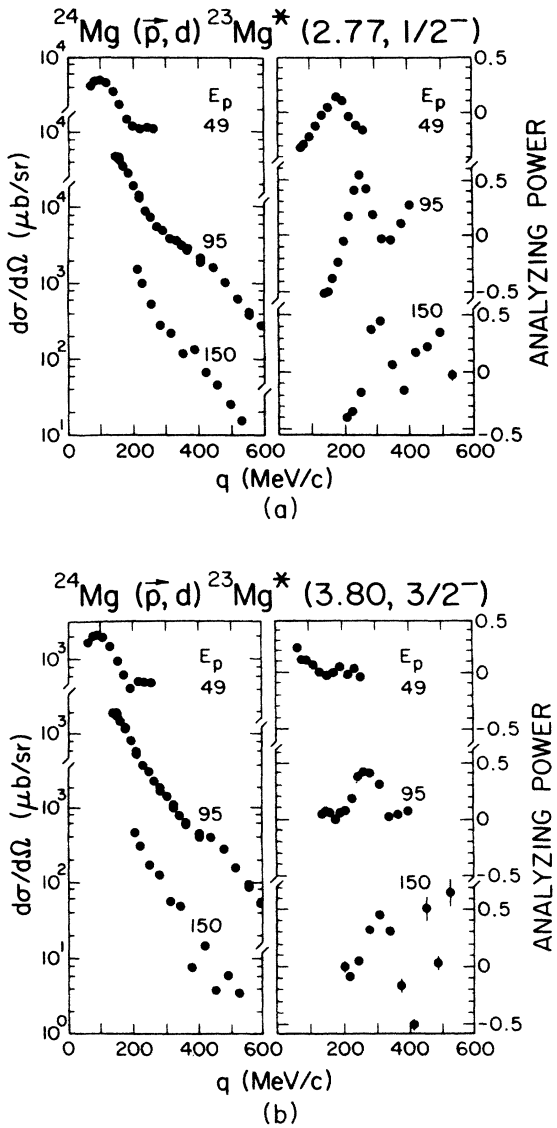

FIG. 2. Differential cross section and analyzing-power angular distributions for two $l_n=1$ transitions to low-lying states in ^{23}Mg. (a) displays the results for the transition to the $\frac{1}{2}^-$ state at 2.77 MeV; a much weaker $\frac{9}{2}^+$ state at 2.71 MeV is not fully resolved. The transition to the $\frac{3}{2}^-$ state at 3.80 MeV is shown in (b). Refer also to the caption for Fig. 1.

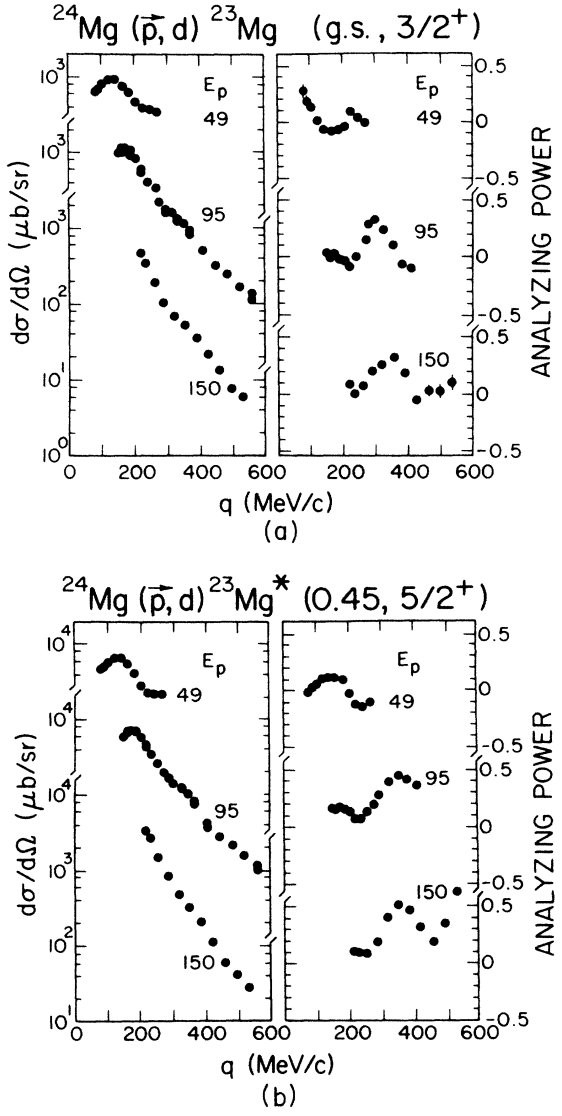

FIG. 3. Differential cross-section and analyzing-power angular distributions for two $l_n=2$ transitions to low-lying states in ^{23}Mg. (a) displays the results for the transition to the $\frac{3}{2}^+$ ground state, and (b) to the $\frac{5}{2}^+$ state at 0.45 MeV. Refer also to the caption for Fig. 1.

at 49 MeV to a maximum of about 0.9 at 95 MeV, and then appears to start to decrease again by 150 MeV. However, the minimum around 30° to 35° does shift to somewhat smaller angles at higher energies.

Figures 2 and 6 show the results for the $l_n=1$ transitions to the $\frac{1}{2}^-$ and $\frac{3}{2}^-$ states. The most striking j-dependent feature of the analyzing powers [the negative result for $\frac{1}{2}^-$ states at forward angles compared to the positive or near-zero result for $\frac{3}{2}^-$ states (Refs. 3 and 5)] again appears to be nearly stable with angle at around 8° c.m., shifting clearly when plotted against momentum transfer. However, the larger-angle oscillations in the analyzing powers shift when plotted versus either θ or q.

Results for the $l_n=2$ transitions to the $\frac{3}{2}^+$ and $\frac{5}{2}^+$ states are plotted in Figs. 3 and 7. In this case the oscilla-

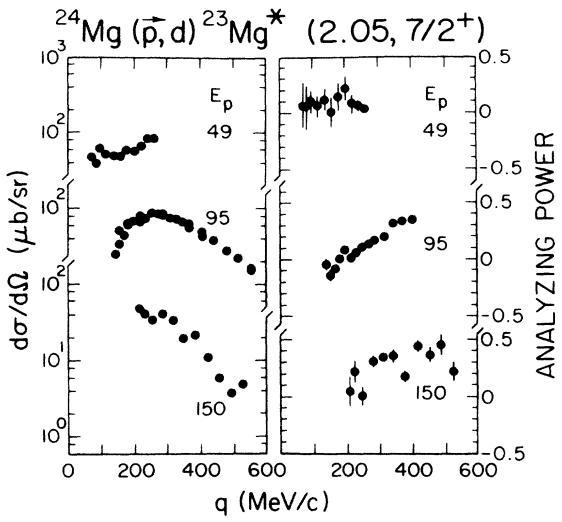

FIG. 4. Differential cross section and analyzing-power angular distributions for the transition to the low-lying $\frac{7}{2}^+$ state in ^{23}Mg. Refer also to the caption for Fig. 1.

tions observed in the analyzing powers are definitely not stable with respect to angle, but are fairly stable with respect to momentum transfer. This diffractionlike behavior is reasonable in view of the better momentum matching and the surface-dominated transition expected in this case.

Figure 4 shows the results for the group leading to the $\frac{7}{2}^+$ state at 2.05 MeV, which is presumed to be excited by

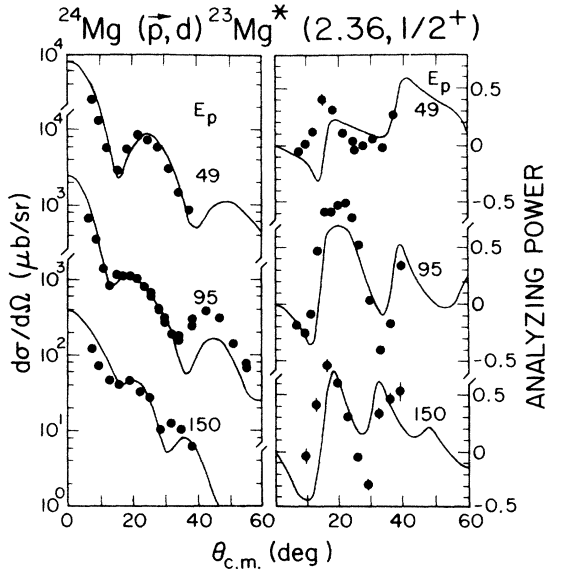

FIG. 5. Comparison of differential cross section and analyzing-power measurements at 49.2, 94.8, and 150.3 MeV bombarding energies for the ($\vec{p}$,d) $l_n=0$ transition to the 2.36-MeV state of ^{23}Mg with exact finite-range distorted-wave calculations using the adiabatic prescription of Ref. 11, as described in the text. The data are the same as displayed in Fig. 1(a) except plotted as a function of center-of-mass angle.

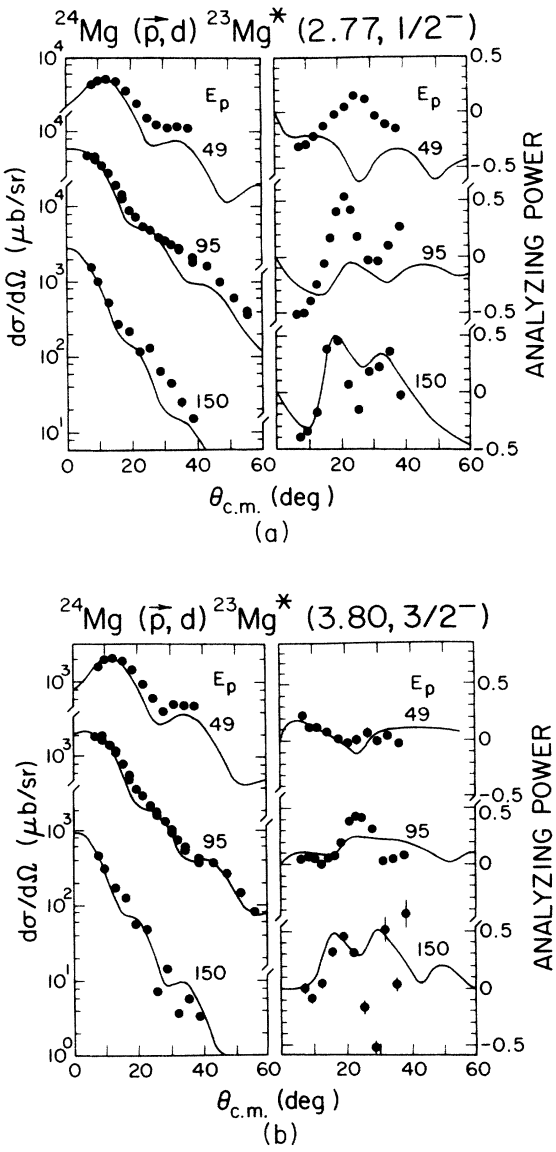

FIG. 6. Comparison of differential cross section and analyzing-power measurements at the three bombarding energies for ($\vec{p}$,d) $l_n=1$ transitions with exact finite-range distorted-wave calculations. (a) shows the comparison for the transition to the $\frac{1}{2}^-$ state at 2.77 MeV, and (b) for the transition to the $\frac{3}{2}^-$ state at 3.80 MeV. Refer also to the caption for Fig. 5.

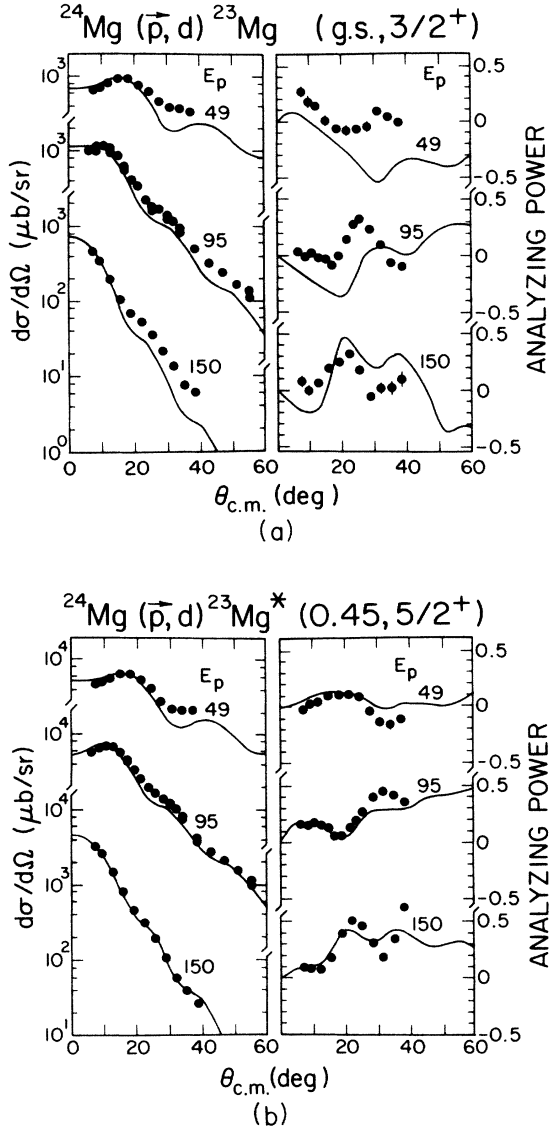

FIG. 7. Comparison of differential cross section and analyzing-power measurements at three bombarding energies for ($\vec{p}$,d) $l_n=2$ transitions with exact finite-range distorted-wave calculations. (a) shows the comparison for the transition to the $\frac{3}{2}^+$ ground state, and (b) for the transition to the $\frac{5}{2}^+$ state at 0.45 MeV. Refer also to the caption for Fig. 5.

a nondirect mechanism. Cross-section angular distributions for such transitions at these energies are characterized by broad maxima,[2] and the analyzing-power results observed here and previously[3] are rather featureless.

IV. EMPIRICAL *j* DEPENDENCE

The *j* dependence of the analyzing powers in stripping or pickup reactions has often been recognized as a method for determining the spins of the residual nuclear states. Unfortunately, at bombarding energies above 35 MeV or so, current theoretical distorted-wave descriptions do not seem to provide realistic predictions of the measured analyzing powers. Nevertheless, observed analyzing-power angular distributions for known transitions have been found to be very useful as "experimental templates" for determining the spins of unknown states. It therefore seems worthwhile to review the empirical mass and energy dependence of the *j* signatures observed in this and previous investigations at energies of 50 MeV and above.

The simplest starting point is to compare the results with the original "sign rule" for (d,p) polarizations for states of the same l_n and different j_n at the same energies. Adapted to the analyzing powers measured in ($\vec{p}$,d) reactions, near the pickup peak the "rule" gave the sign of the analyzing power $A_y(\theta)=\pm$ for $j_n=l_n\pm\frac{1}{2}$. Furthermore,

the ratio of the analyzing powers[19] was expected to be $-(l_n/l_n+1)$ if spin-dependent distortions and the deuteron D state are negligible. Subsequent analyses by Santos,[20,21] and by Johnson *et al.*[22] give a similar result for this ratio, but still under rather restrictive assumptions. Although it is clear that spin-dependent effects are large (for example, they are responsible for the large analyzing powers observed in the $l_n=0$ transitions in Fig. 1), it is interesting to see to what extent the sign rule works at the pickup peak at these higher bombarding energies.

The $l_n=1$ transitions at 49 and 95 MeV shown in Fig. 2, as well as those for deep-hole states excited at 95 MeV in the same reaction,[3] do obey the sign rule at forward angles, although this is only marginally true for one of the four $j_n=l_n+\frac{1}{2}$ measurements at 95 MeV, and the data do not go far enough forward to reach the pickup peak at 150 MeV. Furthermore, $l_n=3$ transitions in heavier nuclei at 95 MeV (Ref. 5) and at 122 MeV (Ref. 23) also obey the sign rule at the pickup peak in 19 cases out of 23; in the exceptions, $A_y(\theta)$ for $j_n=l_n+\frac{1}{2}$ at least is more positive than for $j_n=l_n-\frac{1}{2}$. For the low-lying $l_n=2$ transitions shown in Fig. 3, the sign rule holds at the pickup peak for 49 MeV, and at 95 MeV the analyzing power for $j_n=l_n+\frac{1}{2}$ is more positive than for $j_n=l_n-\frac{1}{2}$; again at 150 MeV the data do not extend over the pickup peak.

In the specific case of $l_n=1$ ($\vec{p}$,d) transitions, the present results, along with those at other energies for other targets, provide evidence on the mass and energy dependence of the $l_n=1$ j signatures. For the ^{13}C($\vec{p}$,d) reaction, the same basic signature shown in Fig. 2 (A_y small and positive for $p_{3/2}$ pickup, and large and negative for $p_{1/2}$ pickup) has been observed at 123 MeV (Ref. 24) and 200 MeV,[25] but the analyzing-power difference disappears by 400 MeV.[25] This characteristic signature also holds at least through 150-MeV bombarding energy for the ^{24}Mg($\vec{p}$,d) reaction reported here (although it is less pronounced at 150 MeV), through 122 MeV for the $\frac{3}{2}^-$ transition in ^{54}Fe($\vec{p}$,d),[23] and at least through 95 MeV for targets of ^{60}Ni and ^{88}Sr.[5] By the time one reaches ^{208}Pb, the characteristic j signature for $l_n=1$ is less pronounced at 95 MeV (Ref. 5) and has disappeared entirely for bombarding energies of 123 MeV.[24]

These results for the energy and mass dependence of the j signatures for $l_n=1$ transfers are qualitatively consistent with the effect of an increased *relative* influence of spin-orbit distortions.[26] For the j dependence to be present it is crucial that the real part of the central potential be large compared to the spin-orbit interaction.[27] As the bombarding energy increases the central part of the proton and deuteron interactions becomes progressively weaker. Although the spin-orbit depth parameter also becomes smaller,[28] the additional factor $\vec{L}\cdot\vec{S}$ roughly compensates so that the effective spin-orbit interaction strength does not change significantly as the energy increases. Thus the forward angle j dependence produced by the simple model[20–22] should eventually disappear as the energy is raised, as in fact is observed in the ($\vec{p}$,d) reaction on carbon by 400 MeV and on lead by 123 MeV. Furthermore, since the $\vec{L}\cdot\vec{S}$ force in both the incident and exit channels will increase with L roughly as kR, the j dependence should disappear as the energy is increased sooner for a heavy nucleus than a light one, just as observed in comparing the results for lead and carbon.

It would be very helpful to have a better physical feeling for the origin of the j-dependent effects observed empirically than one obtains from normal comparisons with distorted-wave calculations. Recent analyses of both vector and tensor polarizations *at large angles* in (d,p) reactions at 79 MeV (Ref. 29) have been able to achieve this in terms of the dominance of "far-side" neutron transfers. However, at the smaller angles emphasized in the present investigation such a simple picture does not appear to be applicable because near-side and far-side amplitudes are comparable and interfere.

V. ADIABATIC APPROXIMATION ANALYSIS

This section describes comparisons between sample distorted-wave calculations with the data at the three bombarding energies employed. Exact finite-range distorted-wave calculations were carried out using the program DWUCK5,[30] applying the adiabatic approximation.[11] A Reid soft-core potential was used for the deuteron wave function. Proton optical-model potential parameters at 50 and 95 MeV were obtained from the prescription of Hatanaka *et al.*[9] This parametrization was also extrapolated to 150 MeV in order to compare predictions with those at this energy by Alons *et al.*,[10] who used proton parameters based upon the impulse approximation. It should be noted that the extrapolation of the Hatanaka prescription up to 150 MeV leads to small values of the real central potential strength (11 MeV compared to 25 MeV for the impulse approximation); the volume imaginary term in this extrapolation is 19 MeV compared to 15 MeV for the impulse approximation.

The adiabatic prescription[11] is intended to take into account breakup effects in the deuteron channel. This procedure requires the combination of proton and neutron parameters evaluated at half the center-of-mass energy. For the proton parameters the prescription due to Hatanaka *et al.*[9] was used. The paucity of information on neutron elastic scattering at the energies of interest here led to the adoption of proton parameters (without the Coulomb term) as the neutron parametrization. The spin-orbit parameter V_{so} was set to -5.6 MeV for these calculations. Nonlocality corrections were included in the exact finite-range calculations, with standard values being used for the proton (0.85 fm), deuteron (0.54 fm), and transferred neutron (0.85 fm).

A bound-state geometry having a diffuseness 0.65 fm was employed, with the spin-orbit parameter λ set at 25. The radii of the bound-state geometries were determined from a prescription for the rms radius value of the valence orbital. Recently Sick *et al.*[31] have shown that precise nucleon radial wave functions, $R(r)$, can be obtained (albeit in a model-dependent way) for a few special cases by combining results from single-nucleon transfer reactions, which yield the tail of $R(r)$, and magnetic electron scattering, which localize the peak of $R^2(r)$ by specifying a root-mean-square radius. It has been demonstrat-

ed that the use of such radial functions in analyses of single-nucleon transfer reactions leads to a more realistic determination of "absolute" spectroscopic factors.[32] Since no experimental rms radii for the orbitals under study are available, values were used from Hartree-Fock calculations for ^{24}Mg employing the Skyrme interaction *SG*II from Van Giai and Sagawa,[33] which gives results in close accord with electron scattering in other cases. These values are 3.294 fm for the $1d_{5/2}$ orbital (yielding a bound-state radius parameter $r_0=1.369$ fm), 3.502 fm for the $2s_{1/2}$ orbital ($r_0=1.628$ fm), 3.591 fm for the $1d_{3/2}$ orbital ($r_0=1.650$ fm), 2.782 fm for the $1p_{3/2}$ orbital ($r_0=1.241$ fm), and 2.776 fm for the $1p_{1/2}$ orbital ($r_0=1.288$ fm).

Within this general framework, the calculations exhibited very little sensitivity of either the angular distribution shapes or the spectroscopic factors to the parameters V_{so} and λ. Utilizing either the extrapolation of the Hatanaka prescription or the impulse approximation at 150 MeV also did not provide predictions with significantly different shapes; however, as discussed below, the spectroscopic factors derived by these two methods at 150 MeV were significantly different.

The curves in Figs. 5 to 7 represent the adiabatic approximation predictions using the Hatanaka extrapolation at 150 MeV and the general framework described in the above paragraphs. It is clear that although the calculations reproduce many gross features, there are substantial shortcomings in the predicted shapes when compared to the data. For example, the analyzing powers for the $j_n=l_n-\frac{1}{2}$ cases are out of phase with the predictions at 49 MeV, but become in phase (though only roughly similar to the predictions) at the higher bombarding energies. The analyzing-power comparisons for the $j_n=l_n+\frac{1}{2}$ cases are generally better for all three energies, except for the 150-MeV results for the $\frac{3}{2}^-$ state at 3.80 MeV.

Spectroscopic factors extracted from a "correct" analysis should be independent of bombarding energy. Table I shows the spectroscopic factors obtained from the comparisons described above, as well as those obtained with the impulse approximation parameters at 150 MeV. For the two $l_n=0$ transitions, the apparent spectroscopic factor increases by a factor of 2 to 2.5 between 49 and 150 MeV when the Hatanaka extrapolation is used. However, employing the impulse approximation parameters at 150 MeV gives spectroscopic factors comparable to those obtained at the lower energies using the Hatanaka prescription. This result agrees with the much more extensive calculations of Alons *et al.*[10] of the $l_n=0$ data. The latter analysis shows essentially no energy dependence of the spectroscopic factor from 27 to 185 MeV when the impulse approximation parameters are used above 95 MeV, and a somewhat larger and more diffuse bound-state geometry than standard is employed. The larger bound-state radii used in the present work (with the rms radius prescription) and in the analysis by Alons *et al.* cause the bound-state wave function to be pushed further away from the nuclear interior, thus reducing the sensitivity to the lower partial waves in the entrance and exit channels.

For the $l_n=1$ cases studied, only a 30–50% increase is seen in the extracted spectroscopic factors from 49 to 95 MeV, with no change or a drop at 150 MeV depending on which proton parameters were used. The spectroscopic factors obtained for the $l_n=2$ transitions vary by 20% or less.

VI. CONCLUSIONS

This experiment provides a data base of differential cross sections and analyzing powers for $l_n=0$, 1, and 2

TABLE I. Spectroscopic factors for the ^{24}Mg(p,d)^{23}Mg reaction obtained using exact-finite-range calculations.

			C^2S_{lj}				
E_x (MeV)	j^π	Assumed l	49.2 MeV (Ref. 9 parameters)	94.8 MeV (Ref. 9 parameters)	150.3 MeV (Ref. 9 parameters)	150.3 MeV (Impulse approximation parameters)	Theory (Ref. 34)
0.00	$\frac{3}{2}^+$	2	0.11	0.12	0.13	0.11	
0.45	$\frac{5}{2}^+$	2	1.5	1.8	1.7	1.4 (1.1)[a]	2.55
2.36	$\frac{1}{2}^+$	0	0.090[b]	0.12[b]	0.23[b]		
2.36	$\frac{1}{2}^+$	0	0.060[c]	0.080[c]	0.14[c]	0.09 (0.10)[a]	0.28
2.77	$\frac{1}{2}^-$	1	1.4	1.8	1.8	1.4	
2.91	$(\frac{3}{2}^+)$	2	0.090	0.095	0.07[d]		
3.80	$\frac{3}{2}^-$	1	0.62	0.95	0.90	0.79	
4.36	$\frac{1}{2}^+$	0	0.036[b]	0.070[b]	0.070[b]		
4.36	$\frac{1}{2}^+$	0	0.025[c]	0.045[c]	0.050[c]	0.037	

[a]Values from Ref. 10 with bound state $r_0=1.385$ fm, $a_0=0.743$ fm.
[b]Fitted at second maximum of cross section angular distribution.
[c]Fitted to initial slope of cross section angular distribution.
[d]Poorly resolved.

transitions in the ^{24}Mg($\vec{p}$,d) reaction at 49 and 150 MeV taken with the same experimental setup, including a check run at 95 MeV for comparison with earlier spectrometer data at that energy. Comparisons with exact finite-range distorted-wave calculations using the adiabatic approximation and an extrapolated proton parametrization used by Hatanaka *et al.*[9] show gross similarities to the data, but some shape discrepancies are apparent, especially for the $j_n = l_n - \frac{1}{2}$ cases at 49 MeV. The energy dependence of the extracted spectroscopic factors within the framework of this comparison is largest for the $l_n = 0$ transitions, becoming less pronounced for $l_n = 1$ and almost disappearing for $l_n = 2$. This observation is consistent with the fact that the $l_n = 0$ transitions more generally seem to cause problems in distorted-wave calculations at these energies, probably due to the increased momentum mismatch which causes difficulties in treating the nuclear interior properly. For the $l_n = 0$ transitions, utilizing proton parameters based upon the impulse approximation at 150 MeV has little effect on the angular distribution shapes, but results in extracted spectroscopic factors more in agreement with those obtained using the Hatanaka prescription at the lower energies.

Using the empirical results of this experiment and other published data, a summary of the known j dependence for (p,d) reactions as a function of target mass and energy was presented. In $l_n = 1$ cases, for which the most data are available, a qualitative explanation was given which is consistent with the observations that the j dependence eventually disappears as the energy is raised, and that this occurs at lower energies for the heavier targets. Within the sparse published data set for $l_n = 1$, 2, and 3 transitions in this energy range, the "sign rule" $A_y(\theta) = \pm$ for $j_n = l_n \pm \frac{1}{2}$ holds at the pickup peak up to 122 MeV for a majority of the cases where the data extend over this peak; in those cases where it fails the analyzing power is more positive for $j_n = l_n + \frac{1}{2}$ than for $j_n = l_n - \frac{1}{2}$.

ACKNOWLEDGMENTS

We would gratefully like to acknowledge numerous discussions of the data and its interpretations with R. C. Johnson, F. D. Santos, J. A. Tostevin, and E. J. Stephenson. Thanks are also due to B. A. Brown for providing the Hartree-Fock calculations for ^{24}Mg. One of us (D.W.M.) appreciates the hospitality accorded by the Kernfysisch Versneller Instituut in Groningen and the University of Surrey where parts of this paper were written. The assistance of W. Lozowski in target preparation, and of the operations and research support staff of the Indiana University Cyclotron Facility, is also gratefully acknowledged. This work was supported in part by National Science Foundation Grant No. PHY 81-14339 and by Department of Energy Contract No. DE-AC02-81-ER-40015.

*Present address: Department of Physics, Princeton University, Princeton, NJ 08544.

[1]J. R. Shepard, E. Rost, and P. D. Kunz, Phys. Rev. C **25**, 1127 (1982).
[2]D. W. Miller, W. P. Jones, D. W. Devins, R. E. Marrs, and J. Kehayias, Phys. Rev. C **20**, 2008 (1979).
[3]D. W. Miller, W. W. Jacobs, D. W. Devins, and W. P. Jones, Phys. Rev. C **26**, 1793 (1982).
[4]G. M. Crawley, J. Kasagi, S. Gales, E. Gerlic, D. Friesel, and A. Bacher, Phys. Rev. C **23**, 1818 (1981).
[5]H. Nann, D. W. Miller, W. W. Jacobs, D. W. Devins, W. P. Jones, and Li Qing-Li, Phys. Rev. C **27**, 1073 (1983).
[6]G. H. Rawitscher and S. N. Mukherjee, Phys. Lett. **110B**, 189 (1982).
[7]R. C. Johnson, N. Austern, and M. H. Lopes, Phys. Rev. C **26**, 348 (1942).
[8]E. Rost, J. R. Shepard, and D. Murdock, Phys. Rev. Lett. **49**, 448 (1982).
[9]K. Hatanaka, M. Fujiwara, K. Hosono, N. Matsuoka, T. Saito, and H. Sakai, Phys. Rev. C **29**, 13 (1984).
[10]P. W. F. Alons, J. J. Kraushaar, D. W. Miller, J. Brown, D. L. Friesel, W. W. Jacobs, W. P. Jones, H. Nann, and P. Pichardo, Phys. Lett. **145B**, 34 (1984).
[11]R. C. Johnson and P. J. R. Soper, Phys. Rev. C **1**, 976 (1970); J. D. Harvey and R. C. Johnson, *ibid.* **3**, 636 (1971).
[12]D. L. Friesel, R. H. Pehl, and B. Flanders, Nucl. Instrum. Methods **207**, 403 (1983).
[13]L. C. Welch, IEEE Trans. Nucl. Sci. **NS-28**, 3758 (1981).
[14]D. A. Low *et al.*, Indiana University Cyclotron Facility Technical and Scientific Report, 1983 (unpublished), p. 156.
[15]R. E. Hindsley and J. T. Meek, Indiana University Cyclotron Facility version FITIT (unpublished).
[16]D. L. Friesel, P. Schwandt, A. Nadasen, G. Caskey, A. Galonsky, and R. E. Warner, Nucl. Instrum. Methods (to be published).
[17]R. E. Carbon *et al.*, Nucl. Instrum. Methods **188**, 465 (1981).
[18]J. Källne and B. Fagerström, Phys. Scr. **11**, 79 (1974).
[19]R. Huby *et al.*, Nucl. Phys. **9**, 94 (1958).
[20]F. D. Santos, Proceedings of the Third International Symposium on Polarization Phenomena in Nuclear Reactions, Madison, 1970, edited by H. H. Barschall and W. Haeberli (University of Wisconsin, Madison, 1971), p. 758.
[21]F. D. Santos, Nucl. Phys. **A236**, 90 (1974).
[22]R. C. Johnson, F. D. Santos, R. C. Brown, A. A. Debenham, G. W. Greenlees, J. A. R. Griffith, O. Karban, D. C. Kocher, and S. Roman, Nucl. Phys. **A208**, 221 (1973).
[23]S. A. Dickey, J. J. Kraushaar, J. R. Shepard, D. W. Miller, W. W. Jacobs, and W. P. Jones, Nucl. Phys. **A441** 189 (1985).
[24]J. J. Kraushaar, J. R. Shepard, D. W. Miller, W. W. Jacobs, W. P. Jones, and D. W. Devins, Nucl. Phys. **A394**, 118 (1983).
[25]R. P. Liljestrand, J. M. Cameron, D. A. Hutcheon, R. Macdonald, W. J. McDonald, C. A. Miller, W. C. Olsen, J. J. Kraushaar, J. R. Shepard, J. G. Rogers, J. R. Tinsley, and C. E. Stronach, Phys. Lett. **99B**, 311 (1981).
[26]R. C. Johnson (private communication).
[27]F. D. Santos (private communication).
[28]See, for example, P. Schwandt, H. O. Meyer, W. W. Jacobs, A. D. Bacher, S. E. Vigdor, M. D. Kaitchuck, and T. R. Donoghue, Phys. Rev. C **26**, 55 (1982).

[29]E. J. Stephenson, V. R. Cupps, J. D. Brown, C. C. Foster, W. P. Jones, D. W. Miller, H. Nann, P. Schwandt, J. W. Seubert, and J. A. Tostevin; also, J. A. Tostevin, R. C. Johnson, E. J. Stephenson, V. R. Cupps, J. D. Brown, C. C. Foster, W. P. Jones, D. W. Miller, H. Nann, P. Schwandt, and J. W. Seubert, Proceedings of the Sixth International Symposium on Polarization Phenomena in Nuclear Physics, Osaka, Japan, 1985, J. Phys. Soc. Jpn. Suppl. (to be published).

[30]P. D. Kunz (unpublished); extended version of J. R. Comfort (unpublished).

[31]I. Sick *et al.*, Phys. Rev. Lett. **38**, 1259 (1977); I. Sick, Comments Nucl. Part. Phys. **9**, 55 (1980).

[32]A. E. L. Dieperink and I. Sick, Phys. Lett. **109B**, 1 (1982).

[33]N. Van Giai and H. Sagawa, Phys. Lett. **106B**, 379 (1981).

[34]B. H. Wildenthal and B. A. Brown (private communication).